ECTI Transactions on Computer and Information Technology
Journal homepage: https://ph01.tci-thaijo.org/index.php/ecticit/
Published by the ECTI Association, Thailand, ISSN: 2286-9131

Detection of Dangerous Motorcycling Using YOLO and Machine Learning Classifiers

Ruixue Si[1] and Rong Phoophuangpairoj[2]

ABSTRACT

The work studied three methods to identify risky motorcycle riding. It aids in identifying risky motorcyclists who adopt unusual riding positions, which lead to a rise in traffic accidents. This work established the feasibility of monitoring hazardous riding on public roadways. We investigated the detection of motorcycle riding types using 1) the motorcycle's extracted images, 2) the motorcyclist's extracted images, and 3) the motorcyclist's pose landmarks. You Only Look Once (YOLO) was applied to detect a motorcycle, a motorcyclist, and the landmarks of a motorcyclist from images. The findings indicated that the classification derived from YOLO-detectable motorcycles surpassed that of the motorcyclists and their pose landmarks. The VGG16 surpassed MobileNet, CNN, and ResNet50 in classifying normal and dangerous riding. YOLO's efficacy in identifying specific pose landmarks at night was insufficient. Detecting dangerous motorcycling based on the motorcyclists' pose landmarks was ineffective at night. Identifying dangerous motorcycling from the detected motorcycles was the most effective. The findings indicated that YOLO attained an accuracy of 71.09% in motorcycle detection from daytime and nighttime images, whereas VGG16 acquired an accuracy of 98.75% in recognizing dangerous motorcycling.

Article information:

Keywords: Machine Learning, Dangerous Motorcycling, Object Detection, Random Forest, Riding Pose Landmarks, YOLO

Article history:
Received: October 17, 2024
Revised: March 22, 2025
Accepted: March 29, 2025
Published: April 26, 2025
(Online)

DOI: 10.37936/ecti-cit.2025192.259018

1. INTRODUCTION

Road safety accidents are a ubiquitous problem around the world. Every year, traffic accidents cause the deaths of thousands of people. Motorcycles are very popular in Thailand and are the most common type of car involved in crashes in most parts of the country. Aside from the deaths caused by motorcycle riders and passengers who neglect to wear helmets during accidents, improper riding can also result in serious or catastrophic injuries. Fig. 1 shows normal and dangerous riding. Recognizing helmets is essential in reducing road accidents. To minimize the injuries suffered by motorcyclists in accidents, researchers studied the methods to detect motorcyclists wearing or not wearing helmets [1]. Jakubec et al. used YOLOv7 to detect a helmet. The model contributed to resolving the issue of detecting helmets on two-wheeled vehicles [2]. Observing motorcyclists' riding poses and prior work is helpful to prevent injuries. Researchers should focus on distinguishing between safe and risky riding.

(a) Normal riding (b) Dangerous riding

Fig. 1: *Normal and Dangerous Riding.*

YOLO covers various vision AI tasks, such as object identification, pose estimation, tracking, and classification. Wearing a helmet guarantees worker safety on construction sites and industries. Built on cutting-edge advances in deep learning and computer vision. Researchers used YOLO to detect helmet-wearing [3], [4]. The field of human posture identification has extensively researched posture detection and other related techniques [5]. Pose land-

[1]The author is with the 1College of Engineering, Rangsit University, Pathum Thani, Thailand, Email: ruixue.s66@rsu.ac.th
[2]The author is with the Department of Computer Engineering, College of Engineering, Rangsit University, Pathum Thani, Thailand, Email: rong.p@rsu.ac.th

marks were also successfully used as features to classify weightlifting phases [6]. YOLO could recognize everyday objects such as persons, cars, and motorcycles. Real-time motorbike detection applied YOLOv5 and achieved high accuracy [7]. The YOLO algorithm could accurately detect human postures such as walking, sitting, and falling [8]. Maji *et al.* (2020) employed the widely used YOLO for 2D multi-person pose estimation on an image, and YOLO-pose achieved new state-of-the-art results on COCO validation [9]. Fig. 2 shows the YOLO pose landmarks of a person. Pose estimation involves identifying the precise coordinates of specific locations within a picture, known as key points. Points can denote object components, such as joints, landmarks, or other notable characteristics, represented using 2D [x, y] coordinates.

This study developed various methodologies using machine learning image classification and pose landmarks to accurately detect safe and risky riding, mitigating accidents and discouraging motorcyclists from engaging in dangerous riding practices.

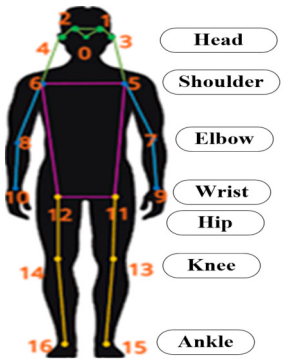

Fig.2: *YOLO Pose Landmarks of a Person.*

2. LITERATURE REVIEW

YOLO can detect objects [1], [2], [3], [6], [8], [9]. Researchers used YOLO to classify tree species [10], [11]. Classifying tree species in transmission line corridors can attain a maximum accuracy of 85.42% in recognizing individual tree species [10]. Additionally, YOLO was applied to detect pine-wilt-disease-affected trees and forest fires [12], [13]. YOLOv5's lightweight architecture enabled effective deployment on edge devices, offering a crucial balance between detection accuracy and processing efficiency for applications like mobile vision systems and drone-based monitoring [14], [15].

Researchers applied Mobilenet to classify images [6], [16]. MobileNet optimally manages the compromise between data processing time and accuracy. MobileNet replaced the traditional convolution filters with two layers, depthwise convolution and pointwise convolution, to reduce feature extraction time. For the classification problems, several experts used simple CNNs [6], [16]. In CNN, the convolutional layers use different filters to find features and make a feature map that accurately shows the input features. CNN initially transforms the characteristics into one-dimensional features and transmits them to a neural network for categorization. VGG16 is a highly advanced convolutional neural network significantly impacting computer vision. It has demonstrated exceptional capabilities in tasks like picture categorization and object detection. VGG16 was applied to classify weeds in paddy fields, and the result showed that the VGG16 model achieved the highest accuracy of around 90% [17]. Researchers also combined VGG16 with other machine learning classifiers to achieve high accuracy in paddy leaf disease classification [18]. ResNet50 is a convolutional neural network comprising 50 layers to classify images [6], [16].

The k-nearest neighbor approach (KNN) is an effective nonparametric classifier that categorizes an unclassified pattern based on the majority class of its k-nearest neighbors. For each new test sample, it calculates the distances between the test sample and all training samples. It selects the "k" nearest training samples from all distances and determines which class contains the most elements within the "k" closest set [19]. Researchers employed KNN to identify drowsiness [20] and classify EMG signals for hand rehabilitation [21]. SVM and ANN were applied to classify weightlifting phases from posture landmarks and achieved accuracy of 91.96% and 89.86%, respectively [6]. An analysis of the user's sitting posture used a pressure-sensing-based device for sitting posture detection. The findings indicated the efficacy of the SVM algorithm in detecting the user's sitting posture [22]. Random forest (RF) is an ensemble machine learning system aggregating many decision trees for a more precise prediction. During the training phase, it functions by creating many decision trees. Every tree is built by utilizing a random portion of the dataset, guaranteeing that each division contains a random selection of features. During the prediction phase, the RF algorithm aggregates the outputs of all the trees by voting. This method, which involves multiple trees contributing their insights, ensures accurate outcomes. Using a single decision tree has drawbacks, such as overfitting and instability [23]. The Random Forest (RF) can handle both regression and classification problems. It can process many high-dimensional features without requiring dimensionality reduction [24], and it sustains good classification accuracy even when missing data exists. The field of road safety has extensively utilized machine learning models, including the RF. The RF was used to develop an accurate predictive model identifying the potential elements influencing fatal falls from height incidents in the Malaysian construction sector. The research demonstrated the viability of machine learn-

ing in construction safety management [25].

3. MATERIALS AND METHODS

3.1 Data

For the image classification experiments, they used 4000 images, including 1000 daytime motorcycle images, 1000 low-light condition motorcycle images, 1000 daytime motorcyclist images, and 1000 low-light condition motorcyclist images. Each set of 1000 images had 700 images depicting regular motorcycle riding and 300 images illustrating dangerous motorcycle riding. YOLO detected all parts of motorcycles and motorcyclists. This study used 1000 daytime and 100 low-light sets of YOLO-detectable pose landmarks. The limited low-light data for motorcyclist pose landmarks resulted from YOLO's insufficient efficacy in detecting them at nighttime. We trained all machine learning classifiers using 80% of the images and tested them using 20% of the images.

3.2 Instruments

YOLOv11 was used to detect motorcycles and motorcyclists. YOLO can detect objects such as persons, bicycles, cars, and motorcycles without training customized models. MobileNet, VGG16, CNN, and ResNet50 classifiers were applied to classify images of motorcycles and those of motorcyclists. In addition, YOLO detected the pose landmarks of a person (motorcyclist) as features for the classification. Scikit-learn was employed to construct KNN, ANN, SVM, and RF classifiers and to assess the outcomes using confusion matrices, precision, recall, F1 score, macro average, and weighted average.

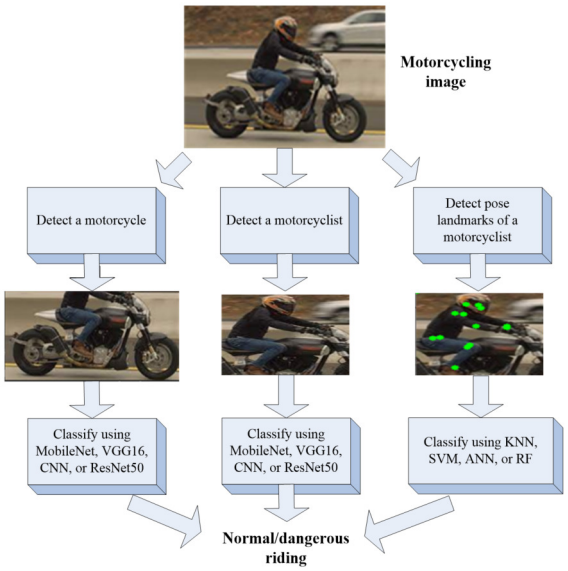

Fig.3: *Proposed Methods for Classifying Normal and Dangerous Riding.*

3.3 Methods

The proposed methods for riding classification based on 1) a detected motorcycle, 2) a detected person, and 3) detected pose landmarks were studied and compared. Fig. 3 shows three methods investigated for detecting dangerous motorcycling.

The first method used YOLO to detect the presence of a motorcycle, and it used the extracted motorcycle images to train and test machine learning classifiers consisting of MobileNet, VGG16, simple CNN, and ResNet50. The second method used YOLO to detect the presence of a motorcyclist, and it used the extracted motorcyclist images to train and test machine learning classifiers. The third method used the pose landmarks detected by YOLO as features. Then, KNN, SVM, ANN, or RF used the features to classify normal riding from dangerous riding. In the experiments, we did not train customized models for detecting motorcycles, motorcyclists, and the motorcyclists' pose landmarks. We employed the YOLO's capabilities for the detection.

Fig. 4 shows examples of detected motorcycles. Fig. 5 and Fig. 6 illustrate examples of detected motorcyclists and their pose landmarks.

Fig.4: *Examples of Detected Motorcycles.*

Fig.5: *Examples of Detected Motorcyclists.*

Fig.6: *Examples of detected motorcyclists' pose landmarks.*

In addition to the pose landmarks YOLO extracted from the motorcyclists, we calculated and applied extended features to distinguish between normal and dangerous riding.

3.3.1 Calculate Extended Features from a Motorcyclist's Pose Landmarks

This part used the extended features computed from 17 pose landmarks (points on a motorcyclist). We added twenty-four features to the original 17 YOLO landmarks, as shown in Table 1. The total number of YOLO features (17×2) and extended features (24) was 58.

Table 1: *Extended Features.*

No.	Extended features
1.	Slope between P5 (Left shoulder) and P7 (Left elbow)
2.	Slope between P6 (Right shoulder) and P8 (Right elbow)
3.	Slope between P7 (Left elbow) and P19 (Left hip)
4.	Slope between P8 (Right elbow) and P10 (Right wrist)
5.	Slope between P5 (Left shoulder) and P11 (Left hip)
6.	Slope between P6 (Right shoulder) and P12 (Right hip)
7.	Slope between P11 (Left hip) and P13 (Left knee)
8.	Slope between P12 (Right hip) and P14 (Right knee)
9.	Slope between P13 (Left knee) and P15 (Left ankle)
10.	Slope between P14 (Right knee) and P16 (Right ankle)
11.	Slope between P11 (Left hip) and P15 (Left ankle)
12.	Slope between P12 (Right hip) and P16 (Right ankle)
13.	Slope between P5 (Left shoulder) and P13 (Left knee)
14.	Slope between P6 (Right shoulder) and P14 (Right knee)
15.	Slope between P5 (Left shoulder) and P15 (Left ankle)
16.	Slope between P6 (Right shoulder) and P16 (Right ankle)
17.	Distance between P5 (Left shoulder) and P9 (Left wrist)
18.	Distance between P6 (Right shoulder) and P10 (Right wrist)
19.	Distance between P9 (Left wrist) and P10 (Right wrist)
20.	Distance between P11 (Left hip) and P15 (Left ankle)
21.	Distance between P12 (Right hip) and P16 (Right ankle)
22.	Distance between P15 (Left ankle) and P16 (Right ankle)
23.	The relative distance between P9 (Left wrist) and P10 (Right wrist)
24.	The relative distance between P15 (Left ankle) and P16 (Right ankle)

This work used Equation 1 to calculate the extended features 1-16, Equation 2 to calculate the extended features 17 to 22, and Equation 2-4 to calculate the extended features 23 and 24.

Given:

(x_i, y_i) is a point (p_i) in YOLO pose landmarks.

(x_j, y_j) is a point (p_j) in YOLO pose landmarks.

i is an index for YOLO pose landmarks (ranging from 0 to 16).

$S_{i,j}$ is a slope between p_i and p_j.

$D_{i,j}$ is a distance between p_i and p_j.

$R_{i,j}$ is a relative distance between p_i and p_j.

$$S_{i,j} = \frac{y_j - y_i}{x_j - x_i} \tag{1}$$

$$D_{i,j} = \sqrt{(x_j - x_i)^2 + (y_j - y_i)^2} \tag{2}$$

$$R_{9,10} = \frac{D_{9,10}}{(D_{5,9} + D_{6,10})} \tag{3}$$

$$R_{15,16} = \frac{D_{15,16}}{(D_{11,15} + D_{12,16})} \tag{4}$$

3.4 Classify Features

We applied four classifiers, MobileNet, VGG16, CNN, and ResNet50, to classify the normal and dangerous riding from images. The top section of the MobileNet featured a global average pooling layer, a dense layer with 128 hidden nodes, a ReLU activation function, and a 0.2 dropout layer. This work applied the efficient classifier VGG16. The top portion of the employed VGG16 consisted of a global average pooling layer, a dense layer with 512 hidden nodes, a ReLU activation function, a 0.1 dropout layer, a dense layer with 64 hidden nodes, a ReLU activation function, and a 0.1 dropout layer. The CNN classifiers consisted of three convolution layers. Each layer employed 32 filters to extract distinctive elements from the images. The flattened layer converted the characteristics into a vector with a single dimension for further classifying using the ANN. The ANN, a component of the CNN, comprised 64 hidden nodes and two output nodes. We employed ResNet-50. The top section of the ResNet-50 featured a global average pooling layer, a dense layer with 64 hidden nodes, a ReLU activation function, a 0.2 dropout layer, a dense layer with 64 hidden nodes, a ReLU activation function, and a 0.2 dropout layer.

For classifying the normal and dangerous riding from pose landmarks, we used KNN classifiers with various k values and SVM classifiers with linear, polynomial, and radial basis kernel functions to classify normal and dangerous riding based on YOLO pose features and their additional features. The classification also used ANNs, modifying the number of hidden layers and nodes. To achieve good outcomes for the ANN classifiers, we set the number of epochs to 150. As for the RF classifiers, we adjusted the number of trees to achieve maximum accuracy in classifying normal and dangerous riding.

4. EXPERIMENTAL RESULTS

4.1 Classification from Daytime Images

4.1.1 Classification from Motorcycle Images Detected by YOLO (Daytime)

This part examined the YOLO-extracted images of motorcycle parts to identify normal and dangerous riding. Table 2 shows the accuracy when using MobileNet, VGG16, CNN, and ResNet50 for riding classification.

Table 2: *Accuracy of Riding Classification from Images of Motorcycles.*

Classifier	Accuracy (%)
MobileNet	97.00
VGG16	99.50
CNN	97.50
ResNet50	95.00

The results showed that the VGG16 classifier outperformed MobileNet, CNN, and ResNet50. Tables

3-10 show the percentage of errors, precision, recall, F1 score, macro average, and weighted average when applying MobileNet, VGG16, CNN, and ResNet50, respectively. When MobileNet was used to classify normal and dangerous riding from the detected motorcycles, it incorrectly classified 10.00% of normal riding as dangerous.

Table 3: *Confusion Matrix of MobileNet Riding Classification from Images of Motorcycles.*

		Classified class	
		Normal riding	Dangerous riding
Actual class	Normal riding	100.00% (140)	0.00% (0)
	Dangerous riding	10.00% (6)	90.00% (54)

Table 4: *Precision, Recall, and F1 Score (%) When Classifying a Motorcycle Using MobileNet.*

Class	Precision (%)	Recall (%)	F1 score (%)	Support
Normal riding	100	90.00	94.74	60
Dangerous riding	95.89	100	97.90	140
macro avg	97.95	95.00	96.32	200
weighted avg	97.12	97.00	96.95	200

As shown in Table 5, VGG16 provided the best accuracy. There was only a 1.67% incorrect classification from normal to dangerous riding without misclassifying dangerous riding as normal. The VGG16 achieved high precision for the normal riding class and high recall for the dangerous riding class.

Table 5: *Confusion Matrix of VGG16 Riding Classification from Images of Motorcycles.*

		Classified class	
		Normal riding	Dangerous riding
Actual class	Normal riding	100.00% (140)	0.00% (0)
	Dangerous riding	1.67% (1)	98.33% (59)

Table 6: *Precision, Recall, and F1 Score (%) When Classifying a Motorcycle Using VGG16.*

Class	Precision (%)	Recall (%)	F1 score (%)	Support
Normal riding	100	98.33	99.16	60
Dangerous riding	99.29	100	99.64	140
macro avg	99.65	99.17	99.40	200
weighted avg	99.50	99.50	99.50	200

Compared to VGG16, the CNN exhibited inferior accuracy, precision, recall, and F1 score for both classes. There was 0.71% of normal riding misclassified as dangerous riding, and 6.67% of dangerous riding misclassified as normal riding.

ResNet50 demonstrated inferior accuracy compared to CNN and VGG16. It misclassified 1.43% of images of normal riding as dangerous riding and 13.33% of images of dangerous riding as normal riding.

Table 7: *Confusion Matrix of CNN Riding Classification from Images of Motorcycles.*

		Classified class	
		Normal riding	Dangerous riding
Actual class	Normal riding	99.29% (139)	0.71% (1)
	Dangerous riding	6.67% (4)	93.33% (56)

Table 8: *Precision, Recall, and F1 Score (%) When Classifying a Motorcycle Using CNN.*

Class	Precision (%)	Recall (%)	F1 score (%)	Support
Normal riding	98.25	93.33	95.73	60
Dangerous riding	97.20	99.29	98.23	140
macro avg	97.72	96.31	96.68	200
weighted avg	97.52	97.50	97.48	200

Table 9: *Confusion Matrix of ResNet50 Riding Classification from Images of Motorcycles.*

		Classified class	
		Normal riding	Dangerous riding
Actual class	Normal riding	98.57% (138)	1.43% (2)
	Dangerous riding	13.33% (8)	86.67% (52)

Table 10: *Precision, Recall, and F1 Score (%) When Classifying a Motorcycle Using ResNet50.*

Class	Precision (%)	Recall (%)	F1 score (%)	Support
Normal riding	96.30	86.67	91.23	60
Dangerous riding	94.52	98.57	96.50	140
macro avg	95.41	92.62	93.87	200
weighted avg	95.05	95.00	94.92	200

The results revealed that using the VGG16 classifier to classify normal and dangerous riding from the extracted motorcycles could provide high accuracy, precision, recall, and F1 score.

4.1.2 Classification from Motorcyclist Images Detected by YOLO (Daytime)

This part investigated the YOLO-extracted images of motorcyclist parts to identify normal and dangerous riding. Table 11 shows the accuracy obtained from four classifiers. VGG16 demonstrated a high accuracy of 99.00% in the riding classification from motorcyclist images.

Table 11: *Accuracy of Riding Classification from Images of Motorcyclists.*

Classifier	Accuracy (%)
MobileNet	98.50
VGG16	99.00
CNN	93.33
ResNet50	94.50

Compared to the VGG16, CNN, and ResNet50 classifiers, the results demonstrated that MobileNet offered comparatively poor accuracy. Tables 12-19 show the percentage of errors, precision, recall, F1 score, macro average, and weighted average when distinguishing normal riding from dangerous riding using images of motorcyclists. The MobileNet misclas-

sified 1.43% of images of normal riding as dangerous riding and 3.34% of images of dangerous riding as normal riding. The normal riding class achieved a precision, recall, and F1 score of 96.67%, and the dangerous riding class achieved a precision, recall, and F1 score of 98.57%.

Table 12: *Confusion Matrix of MobileNet Riding Classification from Images of Motorcyclists.*

		Classified class	
		Normal riding	Dangerous riding
Actual class	Normal riding	98.57% (138)	1.43% (2)
	Dangerous riding	3.34% (2)	96.67% (58)

Table 13: *Precision, Recall, and F1 Score (%) When Classifying a Motorcyclist Using MobileNet.*

Class	Precision (%)	Recall (%)	F1 score (%)	Support
Normal riding	96.67	96.67	96.67	60
Dangerous riding	98.57	98.57	98.57	140
macro avg	97.62	97.62	97.62	200
weighted avg	98.00	98.00	98.00	200

VGG16 delivered much more accurate results than MobileNet. There was an error rate of 0.71% in classifying normal riding as dangerous riding and 1.67% in classifying dangerous riding as normal riding. The normal riding class achieved a precision, recall, and F1 score of 98.33%, and the dangerous riding class achieved a precision, recall, and F1 score of 99.29%.

Table 14: *Confusion Matrix of VGG16 Riding Classification from Images of Motorcyclists.*

		Classified class	
		Normal riding	Dangerous riding
Actual class	Normal riding	99.29% (139)	0.71% (1)
	Dangerous riding	1.67% (1)	98.33% (59)

Table 15: *Precision, Recall, and F1 Score (%) When Classifying a Motorcyclist Using VGG16.*

Class	Precision (%)	Recall (%)	F1 score (%)	Support
Normal riding	98.33	98.33	98.33	60
Dangerous riding	99.29	99.29	99.29	140
macro avg	98.81	98.81	98.81	200
weighted avg	99.00	99.00	99.00	200

Compared to VGG16, the CNN demonstrated inferior accuracy, precision, and F1 score for both classes. There was a 0.71% misclassification rate from normal riding to dangerous riding and a 3.33% misclassification rate from dangerous riding to normal riding.

ResNet50 demonstrated lower accuracy than CNN and VGG16. There was a 3.57% misclassification rate from normal riding to dangerous riding and a 10.00% misclassification rate from dangerous riding to normal riding.

Table 19 shows the precision, recall, F1 score, macro average, and weighted average.

Table 16: *Confusion Matrix of CNN Riding Classification from Images of Motorcyclists.*

		Classified class	
		Normal riding	Dangerous riding
Actual class	Normal riding	99.29% (139)	0.71% (1)
	Dangerous riding	3.33% (2)	96.67% (58)

Table 17: *Precision, Recall, and F1 Score (%) when Classifying a Motorcyclist Using CNN.*

Class	Precision (%)	Recall (%)	F1 score (%)	Support
Normal riding	98.31	96.67	98.33	60
Dangerous riding	98.58	99.29	98.93	140
macro avg	98.44	97.98	98.21	200
weighted avg	98.50	98.50	98.50	200

Table 18: *Confusion Matrix of ResNet50 Riding Classification from Images of Motorcyclists.*

		Classified class	
		Normal riding	Dangerous riding
Actual class	Normal riding	96.43% (135)	3.57% (5)
	Dangerous riding	10.00% (6)	90.00% (54)

Table 19: *Precision, Recall, and F1 Score (%) When Classifying a Motorcyclist Using ResNet50.*

Class	Precision (%)	Recall (%)	F1 score (%)	Support
Normal riding	91.53	90.00	90.76	60
Dangerous riding	95.74	96.43	96.09	140
macro avg	93.64	93.21	93.42	200
weighted avg	94.48	94.50	94.49	200

The results revealed that using the VGG16 classifier to classify normal and dangerous riding from the extracted motorcyclists could provide high accuracy, precision, recall, and F1 score. However, it achieved slightly lower accuracy compared to the classification using motorcycle images.

4.1.3 Classification from YOLO-extracted Motorcyclist Pose Features (Daytime)

The part used the pose features of motorcyclists extracted by YOLO. Four classifiers, KNN, SVM, ANN, and RF, were applied. Table 20 shows the accuracy of riding classification from motorcyclists' YOLO pose features.

When using the YOLO pose features of motorcyclists, the results demonstrated that the RF classifier offered the highest accuracy of 99.50%. Tables 21-28 show the confusion matrices, precision, recall, F1 score, macro average, and weighted average when classifying normal riding from dangerous riding. Tables 21-22 present the confusion matrix, precision, recall, F1 score, macro average, and weighted average of KNN riding classification at peak accuracy.

Tables 23-24 show the confusion matrix, precision, recall, F1 score, macro average, and weighted aver-

Table 20: *Accuracy of Riding Classification from Motorcyclists' YOLO Pose Features.*

Classifier	Accuracy (%)
KNN (k=9)	93.00
KNN (k=11)	92.00
KNN (k=13)	90.50
KNN (k=15)	89.50
SVM (Linear kernel)	93.50
SVM (Polynomial kernel)	91.00
SVM (Radial basis kernel)	95.00
ANN (34-4-2) (1 hidden layer)	88.50
ANN (34-8-2) (1 hidden layer)	90.00
ANN (34-16-2) (1 hidden layer)	87.00
ANN (34-32-2) (1 hidden layer)	91.00
ANN (34-64-2) (1 hidden layer)	90.50
ANN (34-128-2) (1 hidden layer)	87.00
ANN (34-32-32-2) (2 hidden layers)	89.00
ANN (34-64-64-2) (2 hidden layers)	83.50
ANN (34-128-128-2) (2 hidden layers)	90.50
RF (The number of trees = 500)	99.50
RF (The number of trees = 1000)	99.50

Table 21: *Confusion Matrix of KNN Riding Classification from Motorcyclists' YOLO Pose Features.*

		Classified class	
		Normal riding	Dangerous riding
Actual class	Normal riding	100% (140)	0% (0)
	Dangerous riding	23.33% (14)	76.67% (46)

Table 22: *Precision, Recall, and F1 Score (%) When Classifying Motorcyclists' YOLO Pose Features Using KNN.*

Class	Precision (%)	Recall (%)	F1 score (%)	Support
Normal riding	90.91	100	95.24	60
Dangerous riding	100	76.67	86.79	140
macro avg	95.45	88.33	91.02	200
weighted avg	93.64	93.00	92.70	200

age of SVM riding classification when achieving its highest accuracy. There was a 1.43% misclassification rate from normal riding to dangerous riding and a 13.33% misclassification rate from dangerous riding to normal riding.

Table 23: *Confusion Matrix of SVM Riding Classification from Motorcyclists' YOLO Pose Features.*

		Classified class	
		Normal riding	Dangerous riding
Actual class	Normal riding	98.57% (138)	1.43% (2)
	Dangerous riding	13.33% (8)	86.67% (52)

Table 24: *Precision, Recall, and F1 Score (%) When Classifying Motorcyclists' YOLO Pose Features Using SVM.*

Class	Precision (%)	Recall (%)	F1 score (%)	Support
Normal riding	94.52	98.57	96.50	60
Dangerous riding	96.30	86.67	91.23	140
macro avg	95.41	92.62	93.87	200
weighted avg	95.05	95.00	94.92	200

When achieving its highest accuracy, tables 25-26 show the confusion matrix, precision, recall, F1 score, macro average, and weighted average of ANN riding classification. There was a 2.86% misclassification rate from normal riding to dangerous riding and a 23.33% misclassification rate from dangerous riding to normal riding. The recall rate for the normal riding class was just 76.67%.

Table 25: *Confusion Matrix of ANN Riding Classification from Motorcyclists' YOLO Pose Features.*

		Classified class	
		Normal riding	Dangerous riding
Actual class	Normal riding	97.14% (136)	2.86% (4)
	Dangerous riding	23.33% (14)	76.67% (46)

Table 26: *Precision, Recall, and F1 Score (%) When Classifying Motorcyclists' YOLO Pose Features Using ANN.*

Class	Precision (%)	Recall (%)	F1 score (%)	Support
Normal riding	90.67	97.14	93.79	60
Dangerous riding	92.00	76.67	83.64	140
macro avg	91.33	86.90	88.71	200
weighted avg	91.07	91.00	90.75	200

Tables 27-28 show the confusion matrix, precision, recall, F1 score, macro average, and weighted average of the RF classification at its highest accuracy. The RF classifier misclassified 1.67% of images of dangerous riding as normal riding.

Table 27: *Confusion Matrix of RF Riding Classification from Motorcyclists' YOLO Pose Features.*

		Classified class	
		Normal riding	Dangerous riding
Actual class	Normal riding	100% (140)	0% (0)
	Dangerous riding	1.67% (1)	98.33% (59)

Table 28: *Precision, Recall, and F1 Score (%) When Classifying Motorcyclists' YOLO Pose Features Using RF.*

Class	Precision (%)	Recall (%)	F1 score (%)	Support
Normal riding	99.92	100	99.64	60
Dangerous riding	100	98.33	99.16	140
macro avg	99.65	99.17	99.40	200
weighted avg	99.50	99.50	99.50	200

4.1.4 Classification from YOLO-extracted Motorcyclist Pose Features and the Extended Features (Daytime)

In this part, the classification used the pose features of motorcyclists extracted by YOLO and their extended features. Table 29 shows the accuracy of riding classification using KNN, SVM, ANN, and RF. The results indicate that the RF classifiers using

YOLO-extracted motorcyclist posture features and the extended features did not perform better than those using only YOLO-extracted motorcyclist posture features.

Table 29: *Accuracy of Riding Classification from YOLO-Extracted Motorcyclist Pose Features and the Extended Features.*

Classifier	Accuracy (%)
KNN (k=9)	91.50
KNN (k=11)	90.50
KNN (k=13)	89.50
KNN (k=15)	89.50
SVM (Linear kernel)	94.00
SVM (Polynomial kernel)	90.50
SVM (Radial basis kernel)	96.50
ANN (58-16-2) (1 hidden layer)	91.50
ANN (58-32-2) (1 hidden layer)	94.50
ANN (58-64-2) (1 hidden layer)	93.50
ANN (58-128-2) (1 hidden layer)	93.50
ANN (58-16-16-2) (2 hidden layers)	92.50
ANN (58-32-32-2) (2 hidden layers)	76.00
ANN (58-64-64-2) (2 hidden layers)	94.00
ANN (58-128-128-2) (2 hidden layers)	91.00
RF (The number of trees = 500)	99.50
RF (The number of trees = 1000)	99.50

Tables 30-31 show the confusion matrix, precision, recall, F1 score, macro average, and weighted average when using KNN (k=9). The KNN classifier could not achieve high accuracy. It misclassified 28.33% of images of dangerous riding as normal riding.

Table 30: *Confusion Matrix of KNN Riding Classification From YOLO-Extracted Motorcyclist Pose Features and the Extended Features.*

		Classified class	
		Normal riding	Dangerous riding
Actual class	Normal riding	100% (140)	0% (0)
	Dangerous riding	28.33% (17)	71.67% (43)

Table 31: *Precision, Recall, and F1 Score (%) When Classifying Motorcyclists' YOLO Pose Features and the Extended Features Using KNN.*

Class	Precision (%)	Recall (%)	F1 score (%)	Support
Normal riding	89.17	100	94.28	60
Dangerous riding	100	71.67	83.50	140
macro avg	94.59	85.83	88.89	200
weighted avg	92.42	91.50	91.04	200

Tables 32-33 show the confusion matrix, precision, recall, F1 score, macro average, and weighted average when using SVM. Compared to KNN, the SVM achieved better accuracy, precision, and recall rates.

Tables 34-35 show the confusion matrix, precision, recall, F1 score, macro average, and weighted average when using ANN.

Tables 36-37 show the confusion matrix, precision, recall, F1 score, macro average, and weighted average when using the RF classifier. There was a 1.67% misclassification rate from dangerous riding to normal riding. The classification achieved precision, recall, and F1 scores higher than 98% for both classes.

Table 32: *Confusion Matrix of SVM Riding Classification from YOLO-Extracted Motorcyclist Pose Features and the Extended Features.*

		Classified class	
		Normal riding	Dangerous riding
Actual class	Normal riding	98.57% (138)	1.43% (2)
	Dangerous riding	8.33% (5)	91.67% (55)

Table 33: *Precision, Recall, and F1 Score (%) When Classifying Motorcyclists' YOLO Pose Features and the Extended Features Using SVM.*

Class	Precision (%)	Recall (%)	F1 score (%)	Support
Normal riding	96.50	98.57	97.53	60
Dangerous riding	96.49	91.67	94.02	140
macro avg	96.50	95.12	95.77	200
weighted avg	96.50	96.50	96.47	200

Table 34: *Confusion Matrix of ANN Riding Classification from YOLO-extracted Motorcyclist Pose Features and the Extended Features.*

		Classified class	
		Normal riding	Dangerous riding
Actual class	Normal riding	97.86% (137)	2.14% (3)
	Dangerous riding	13.33% (8)	86.67% (52)

Table 35: *Precision, Recall, and F1 Score (%) When Classifying Motorcyclists' YOLO Pose Features and the Extended Features Using ANN.*

Class	Precision (%)	Recall (%)	F1 score (%)	Support
Normal riding	94.48	97.86	96.14	60
Dangerous riding	94.55	86.67	90.43	140
macro avg	94.51	92.26	93.29	200
weighted avg	94.50	94.50	94.43	200

Table 36: *Confusion Matrix of RF Riding Classification from YOLO-extracted Motorcyclist Pose Features and the Extended Features.*

		Classified class	
		Normal riding	Dangerous riding
Actual class	Normal riding	100% (140)	0% (0)
	Dangerous riding	1.67% (1)	98.33% (59)

Table 37: *Precision, Recall, and F1 Score (%) When Classifying Motorcyclists' YOLO Pose Features and the Extended Features Using RF.*

Class	Precision (%)	Recall (%)	F1 score (%)	Support
Normal riding	99.92	100	99.64	60
Dangerous riding	100	98.33	99.16	140
macro avg	99.65	99.17	99.40	200
weighted avg	99.50	99.50	99.50	200

4.2 Classification from Low-light Condition Images

This part used low-light condition images and applied the YOLO to detect motorcycles and motorcyclists and pose landmarks for motorcyclists. Subsequently, we used the detected results to train and classify the dangerous riding.

4.2.1 Classification from Motorcycle Images Detected by YOLO

This part examined the YOLO-extracted images of motorcycle parts to identify normal and dangerous riding. Table 38 shows riding classification accuracy from motorcycle images when using MobileNet, VGG16, CNN, and ResNet50. The classification using VGG16 outperformed MobileNet, a simple CNN, and ResNet50.

Table 38: *Accuracy of Riding Classification from Images of Motorcycles.*

Classifier	Accuracy (%)
MobileNet	98.50
VGG16	100.00
CNN	97.00
ResNet50	95.50

Table 39 shows the confusion matrix of VGG16 riding classification from images of motorcycles. Table 40 shows the confusion matrix, precision, recall, F1 score, macro average, and weighted average when using VGG16.

Table 39: *Confusion Matrix of VGG16 Riding Classification from Images of Motorcycles.*

		Classified class	
		Normal riding	Dangerous riding
Actual class	Normal riding	100.00% (140)	0.00% (0)
	Dangerous riding	0% (0)	100.00% (60)

Table 40: *Precision, Recall, and F1 Score (%) When Classifying a Motorcycle Using VGG16.*

Class	Precision (%)	Recall (%)	F1 score (%)	Support
Normal riding	100	100	100	60
Dangerous riding	100	100	100	140
macro avg	100	100	100	200
weighted avg	100	100	100	200

4.2.2 Classification from Motorcyclist Images Detected by YOLO

This part examined the YOLO-extracted images of motorcycle parts to identify normal and dangerous riding.Table 41 shows the accuracy of riding classification from Images of Motorcyclists when using MobileNet, VGG16, CNN, and ResNet50. Table 42 shows the confusion matrix of VGG16 riding classification from images of motorcyclists.

Table 41: *Accuracy of Riding Classification from Images of Motorcyclists.*

Classifier	Accuracy (%)
MobileNet	97.50
VGG16	98.00
CNN	92.50
ResNet50	91.00

Table 42: *Confusion Matrix of VGG16 Riding Classification from Images of Motorcyclists.*

		Classified class	
		Normal riding	Dangerous riding
Actual class	Normal riding	99.29% (139)	0.71% (1)
	Dangerous riding	5.00% (3)	95.00% (57)

Table 43 shows the confusion matrix, precision, recall, F1 score, macro average, and weighted average when using VGG16.

Table 43: *Precision, Recall, and F1 Score (%) When Classifying a Motorcycle Using VGG16.*

Class	Precision (%)	Recall (%)	F1 score (%)	Support
Normal riding	98.28	95.00	96.61	60
Dangerous riding	97.89	99.29	98.58	140
macro avg	98.08	97.14	97.60	200
weighted avg	98.00	98.00	97.99	200

4.2.3 Classification from YOLO-extracted Motorcyclist Pose Features

Table 44 shows the accuracy of riding classification based on motorcyclists' YOLO pose features when using KNN, SVM, ANN, and RF. The classification accuracy using YOLO motorcyclist pose features appeared relatively high because the experiments used YOLO-detectable images, but the actual performance of this approach was poor due to YOLO's inability to detect the pose landmarks of motorcyclists in low-light conditions efficiently.

Table 44: *Accuracy of Riding Classification from Motorcyclists' YOLO Pose Features.*

Classifier	Accuracy (%)
KNN (k=9)	80.00
KNN (k=11)	80.00
KNN (k=13)	80.00
KNN (k=15)	80.00
SVM (Linear kernel)	80.00
SVM (Polynomial kernel)	80.00
SVM (Radial basis kernel)	90.00
ANN (34-4-2) (1 hidden layer)	90.00
ANN (34-8-2) (1 hidden layer)	85.00
ANN (34-16-2) (1 hidden layer)	75.00
ANN (34-32-2) (1 hidden layer)	80.00
ANN (34-64-2) (1 hidden layer)	85.00
ANN (34-128-2) (1 hidden layer)	85.00
ANN (34-32-32-2) (2 hidden layers)	80.00
ANN (34-64-64-2) (2 hidden layers)	80.00
ANN (34-128-128-2) (2 hidden layers)	90.00
RF (The number of trees = 500)	80.00
RF (The number of trees = 1000)	85.00

Tables 45-46 show the confusion matrix, precision, recall, F1 score, macro average, and weighted average for the classification using motorcyclists' YOLO pose features.

Table 45: *Confusion Matrix of ANN(34-128-128-2) Riding Classification from Motorcyclists' YOLO Pose Features.*

		Classified class	
		Normal riding	Dangerous riding
Actual class	Normal riding	100% (16)	0% (0)
	Dangerous riding	50.00% (2)	50.00% (2)

Table 46: *Precision, Recall, and F1 Score (%) When Classifying Motorcyclists' YOLO Pose Features Using ANN (34-128-128-2).*

Class	Precision (%)	Recall (%)	F1 score (%)	Support
Normal riding	88.89	100	94.12	16
Dangerous riding	100	50.00	66.67	4
macro avg	94.44	75.00	80.39	20
weighted avg	91.11	90.00	88.63	20

4.2.4 Classification from YOLO-extracted Motorcyclist Pose Features and the Extended Features

We applied four classifiers, namely KNN, SVM, ANN, and RF, for riding classification based on YOLO-extracted motorcyclist pose features and extended features. Table 47 shows the accuracy of riding classification from YOLO-extracted motorcyclist pose features and the extended features. This approach provided low accuracy in real situations because of YOLO's inadequate ability to detect the pose landmarks of motorcyclists in low-light conditions.

Table 47: *Accuracy of Riding Classification from YOLO-Extracted Motorcyclist Pose Features and the Extended Features.*

Classifier	Accuracy (%)
KNN (k=9)	80.00
KNN (k=11)	80.00
KNN (k=13)	80.00
KNN (k=15)	80.00
SVM (Linear kernel)	80.00
SVM (Polynomial kernel)	80.00
SVM (Radial basis kernel)	80.00
ANN (58-16-2) (1 hidden layer)	90.00
ANN (58-32-2) (1 hidden layer)	75.00
ANN (58-64-2) (1 hidden layer)	80.00
ANN (58-128-2) (1 hidden layer)	90.00
ANN (58-16-16-2) (2 hidden layers)	85.00
ANN (58-32-32-2) (2 hidden layers)	90.00
ANN (58-64-64-2) (2 hidden layers)	85.00
ANN (58-128-128-2) (2 hidden layers)	90.00
RF (The number of trees = 500)	90.00
RF (The number of trees = 1000)	85.00

Tables 48-49 show the confusion matrix, precision, recall, F1 score, macro average, and weighted average when using RF riding classification from YOLO-extracted motorcyclist pose features and the extended features.

Table 48: *Confusion Matrix of RF Riding Classification from YOLO-Extracted Motorcyclist Pose Features and the Extended Features.*

		Classified class	
		Normal riding	Dangerous riding
Actual class	Normal riding	100% (16)	0% (0)
	Dangerous riding	50.00% (2)	50.00% (2)

Table 49: *Precision, Recall, and F1 Score (%) When Classifying Motorcyclists' YOLO Pose Features and the Extended Features Using RF.*

Class	Precision (%)	Recall (%)	F1 score (%)	Support
Normal riding	88.89	100	94.12	16
Dangerous riding	100	50.00	66.67	4
macro avg	94.44	75.00	80.39	20
weighted avg	91.11	90.00	88.63	20

4.3 Classification from Daytime and Low-light Condition Images

This part examined the YOLO-extracted images of motorcycle parts to identify normal and dangerous riding. Table 50 presents the outcomes of MobileNet, VGG16, CNN, and ResNet50 classifiers. We trained and evaluated all classifiers using images captured in daytime and low-light conditions. The findings demonstrate that VGG16 attained a maximum accuracy of 98.75%.

Table 50: *Accuracy of Riding Classification from Images of Motorcycles.*

Classifier	Accuracy (%)
MobileNet	95.50
VGG16	98.75
CNN	97.00
ResNet50	91.75

Tables 51-52 show the confusion matrix, precision, recall, F1 score, macro average, and weighted average when using VGG16.

Table 51: *Confusion Matrix of VGG16 Riding Classification from Images of Motorcycles.*

		Classified class	
		Normal riding	Dangerous riding
Actual class	Normal riding	100.00 (280)	0% (0)
	Dangerous riding	0.83% (1)	9.17% (119)

The findings indicate that integrating motorcycle detection via YOLO and classification through VGG16 is a practical approach for identifying dangerous motorcycling. The system's performance relied on the YOLO motorcycle detection part and the classification of the normal and dangerous motorcycling parts. Table 53 displays the total number of

Table 52: *Precision, recall, and F1 score (%) when classifying a motorcycle using VGG16.*

Class	Precision (%)	Recall (%)	F1 score (%)	Support
Normal riding	100	99.17	99.58	120
Dangerous riding	99.64	100	99.82	280
macro avg	99.82	99.58	99.70	400
weighted avg	99.75	99.75	99.75	400

motorcycles in images (N), deletion errors (D), substitution errors (S), insertion errors (I), and the accuracy of YOLO motorcycle detection. When using the YOLO11s model with the confidence level (conf) = 0.25 and intersection over union (IoU) = 0.7, YOLO attained an accuracy of 71.09%. YOLO could detect motorcycles during the daytime rather well; however, its performance diminished in low-light conditions or at night. The deletion errors occurred when the system could not detect motorcycles, while the insertion errors occurred when the system detected other objects, such as bicycles, as motorcycles. There was no substitution error because we configured YOLO to detect only motorcycles. The number of images used was 512, and YOLO could detect 400 motorcycles correctly. There were 112 deletions, zero substitutions, and 36 insertion errors. Based on the results in Table 53, which showed that 436 images of motorcycles could be found (512-112+36), the system was about 91.51% accurate at detecting normal and dangerous motorcycling from those detected images. To determine the accuracy, we divided (N - D + I) - (I + the number of misclassifications using VGG16 in Table 51) by (N - D + I).

Table 53: *YOLO Motorcycle Detection Accuracy.*

	N	D	S	I	Accuracy (%)
Daytime normal riding	140	0	0	0	100
Daytime dangerous riding	63	3	0	6	85.71
Nighttime normal riding	218	78	0	13	58.26
Nighttime dangerous riding	91	31	0	17	47.25
Daytime and Nighttime riding	**512**	**112**	**0**	**36**	**71.09**

5. DISCUSSION AND CONCLUSION

This study developed a novel approach to distinguish between dangerous and typical motorcycle riding, which observes driving activities and fills the gap in monitoring potentially hazardous actions on the road. This work has the potential to identify instances of single-wheeled motorcycle riding and riding while lying down, which happens on some streets. The methods used object detection to detect motorcycles and motorcyclists. Although YOLO could detect the pose landmarks of riders, acquiring the riders' landmarks from nocturnal images proved challenging. Among MobileNet, VGG16, simple CNN, ResNet50, SVM, ANN, and RF classifiers, VGG16 achieved the best accuracy for identifying normal and dangerous riding using YOLO-detected motorcycles. The detection accuracy was relatively high for the daytime images. However, the YOLO poorly detected the landmarks during the nighttime. Therefore, employing this method at night diminished the system's performance. Including the extended features did not considerably enhance the accuracy compared to using only YOLO's pose landmarks. In the future, researchers should compare our proposed method with those developed using MediaPipe and investigate methods such as explainable artificial intelligence (XAI) [26] to find important features for the riding classification. To improve detection performance, especially at night, we should investigate using customized models in addition to YOLO pretrained models. This work used a relatively small dataset for training and testing the classifiers, and it focused on single motorcycles. Future studies should add images to the training and testing processes to improve detection and classification. Furthermore, observing accidents when riders fall off their motorcycles and athletes train in a gym is intriguing.

AUTHOR CONTRIBUTIONS

Conceptualization, R. Phoophuangpairoj and R. Si; methodology, R. Phoophuangpairoj and R. Si; software, R. Si and R. Phoophuangpairoj; validation, R. Si and R. Phoophuangpairoj; formal analysis, R. Si and R. Phoophuangpairoj; investigation, R. Si and R. Phoophuangpairoj; data curation, R. Si; writing—original draft preparation, R. Phoophuangpairoj and R. Si; writing—review and editing, R. Phoophuangpairoj and R. Si; visualization, R. Si and R. Phoophuangpairoj; supervision, R. Phoophuangpairoj; funding acquisition, R. Phoophuangpairoj. All authors have read and agreed to the published version of the manuscript.

References

[1] Y. Jamtsho, P. Riyamongkol and R. Waranusast, "Real-time license plate detection for non-helmeted motorcyclist using YOLO," *ICT Express*, vol. 7, no. 1, pp. 104–109, Mar. 2021.

[2] M. Jakubec, E. Lieskovska, A. Brezani and J. Tothova, "Deep Learning-Based Automatic Helmet Recognition for Two-wheeled Road Safety," *Transportation Research Procedia*, vol. 74, pp. 1171–1178, Jan. 2023.

[3] H. Li, D. Wu, W. Zhang and C. Xiao, "YOLO-PL: Helmet wearing detection algorithm based on improved YOLOv4," *Digital Signal Processing*, vol. 144:104283, pp. 1–11, Jan. 2024.

[4] Y. Liu, B. Jiang, H. He, Z. Chen and Z. Xu, "Helmet wearing detection algorithm based on

improved YOLOv5," *Scientific Reports*, vol. 14, no. 1:8768, pp. 1–11, Apr. 2024.

[5] Y. Jiang, R. Hang, Y. Wu, W. Huang, X. Pan and Z. Tao, "Design and Development of Posture Detection System Based on YOLO - OpenPose," in *2023 19th International Conference on Natural Computation, Fuzzy Systems and Knowledge Discovery (ICNC-FSKD)*, pp. 1–7, Jul. 2023.

[6] M. Qi and R. Phoophuangpairoj, "Classification of Snatch Weightlifting Phases," in *2024 12th International Electrical Engineering Congress (iEECON)*, pp. 1–5, Mar. 2024.

[7] A. Akhtar, R. Ahmed, M. H. Yousaf and S. A. Velastin, "Real-Time Motorbike Detection: AI on the Edge Perspective," *Mathematics*, vol. 12, no. 7, 2024.

[8] Y. Shu and L. Hu, "A Vision-based human posture detection Approach for Smart Home Applications," *International Journal of Advanced Computer Science and Applications*, vol. 14, no. 10, pp. 209–216, Jan. 2023.

[9] D. Maji, S. Nagori, M. Mathew and D. Poddar, "YOLO-pose: Enhancing YOLO for multi-person pose estimation using object keypoint similarity Loss," in *IEEE/CVF Conference on Computer Vision and Pattern Recognition Workshops (CVPRW)*, New Orleans, LA, USA, pp. 2636–2645, 2022.

[10] S. Xu, R. Wang, W. Shi and X. Wang, "Classification of Tree Species in Transmission Line Corridors Based on YOLO v7," *Forests*, vol. 15, no. 1, pp. 1–17, 2024.

[11] Y. Liu, Q. Zhao, X. Wang, Y. Sheng, W. Tian and Y. Ren, "A tree species classification model based on improved YOLOv7 for shelterbelts," *Frontiers in Plant Science*, vol. 14, pp. 1–16, Jan. 2024.

[12] X. Zhu *et al.*, "Detection of Pine-Wilt-Disease-Affected Trees Based on Improved YOLO v7," *Forests*, vol. 15, no. 4, pp. 1–18, 2024.

[13] S. Wang *et al.*, "Forest Fire Detection Based on Lightweight Yolo," in *2021 33rd Chinese Control and Decision Conference (CCDC)*, pp. 1560–1565, May 2021.

[14] I. Atik, "CB-YOLOv5: Enhancing drone detection with BottleneckCSP and cross convolution for improved performance," *Journal of Radiation Research and Applied Sciences*, vol. 16, no. 4:100705, pp. 1–5, Dec. 2023.

[15] P. Zhang, X. Liu, J. Yuan and C. Liu, "YOLO5-spear: A robust and real-time spear tips locator by improving image augmentation and lightweight network for selective harvesting robot of white asparagus," *Biosystems Engineering*, vol. 218, pp. 43–61, Jun. 2022.

[16] X. Dong and R. Phoophuangpairoj, "Mango Maturity Classification using VGG16," in *2024 12th International Electrical Engineering Congress (iEECON)*, pp. 1–5, Mar. 2024.

[17] R. Kamath, M. Balachandra, A. Vardhan and U. Maheshwari, "Classification of Weeds of Paddy Fields using Deep Learning," *ECTI Transactions on Computer and Information Technology*, vol. 16, no. 4, pp. 365–377, Dec. 2022.

[18] B. Sowmiya, K. Saminathan and M. Chithra Devi, "An Ensemble of Transfer Learning based InceptionV3 and VGG16 Models for Paddy Leaf Disease Classification," *ECTI Transactions on Computer and Information Technology*, vol. 18, no. 1, pp. 89–100, Jan. 2024.

[19] A. Subasi and S. A. Qureshi, "Chapter 6 - Artificial intelligence-based skin cancer diagnosis," in *Applications of Artificial Intelligence in Medical Imaging*, A. Subasi, Ed., Academic Press, pp. 183–205, 2023.

[20] L. Rahunathan, D. Sivabalaselvamani, M. Pandieswari, S. Priyadharshin and K. Sownthar, "Drowsiness Detection and Accident Prevention by using K Nearest Neighbor (KNN) Algorithm," in *2023 International Conference on Innovative Data Communication Technologies and Application (ICIDCA)*, pp. 575–580, Mar. 2023.

[21] S. Briouza, H. Gritli, N. Khraief, S. Belghith and D. Singh, "EMG Signal Classification for Human Hand Rehabilitation via Two Machine Learning Techniques: kNN and SVM," in *2022 5th International Conference on Advanced Systems and Emergent Technologies (IC_ASET)*, pp. 412–417, Mar. 2022.

[22] M.-C. Tsai, E. T.-H. Chu and C.-R. Lee, "An Automated Sitting Posture Recognition System Utilizing Pressure Sensors," *Sensors*, vol. 23, no. 13, pp. 1–21, 2023.

[23] D. Wu, Y. Zhang and Q. Xiang, "Geographically weighted random forests for macro-level crash frequency prediction," *Accident Analysis & Prevention*, vol. 194:107370, pp. 1–12, Jan. 2024.

[24] J. Yang, S. Han and Y. Chen, "Prediction of traffic accident severity based on random forest," *Journal of Advanced Transportation*, vol. 2023, no. 1:7641472, pp. 1–8, Jan. 2023.

[25] A. Zermane, M. Z. Mohd Tohir, H. Zermane, M. R. Baharudin and H. Mohamed Yusoff, "Predicting fatal fall from heights accidents using random forest classification machine learning model," *Safety Science*, vol. 159:106023, pp. 1–10, Mar. 2023.

[26] C. Dindorf, O. Ludwig, S. Simon, S. Becker and M. Fröhlich, "Machine Learning and Explainable Artificial Intelligence Using Counterfactual Explanations for Evaluating Posture Parameters.," *Bioengineering (Basel)*, vol. 10, no. 5:511, pp. 1–16, Apr. 2023.

Ruixue Si received his B.Sc. degree in computer science from the College of Arts, Media, and Technology, Chiang Mai University. He is now pursuing his master's degree in electrical and computer engineering at the College of Engineering, Rangsit University, Thailand. His research interests include image classification, machine learning, and object detection.

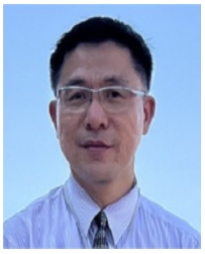

Rong Phoophuangpairoj is an associate professor in the Department of Computer Engineering, College of Engineering, Rangsit University, Thailand. He received a B.Eng. degree in computer engineering from Chulalongkorn University. He also received the M.Sc. and Ph.D. degrees in computer science from Mahidol University. His research interests include signal and image classification, machine learning, object detection, and applied computer applications.